ARTICLES

Free Energy of Oxidation of Metal Aqua Ions by an Enforced Change of Coordination†

Jochen Blumberger and Michiel Sprik*

University Chemical Laboratory, Lensfield Road, Cambridge CB2 1EW, United Kingdom

Received: September 2, 2003; In Final Form: December 6, 2003

A new thermodynamic integration method is introduced to calculate the free-energy difference between the reactant (reduced species) and product (oxidized species) of an electrochemical half reaction. The redox reaction is enforced by a controlled change of a suitable structural characteristic (order parameter) of the solvent coordination. The potential energy surface (PES) of the redox system is constructed from the PESs of the reduced and oxidized states shifted relative to each other by a constant energy μ. As shown in a previous publication (Tavernelli, I.; Vuilleumier, R.; Sprik, M. *Phys. Rev. Lett.* **2002**, *88*, 213002), this potential can be interpreted as the effective potential experienced by the nuclear degrees of freedom in an open system exchanging electrons with a reservoir at fixed electronic chemical potential μ. The method is applied to the half reaction $Ag^{+}_{aq} \rightarrow Ag^{2+}_{aq} + e^{-}$ using constrained Car−Parrinello molecular dynamics simulation. The order parameter (constraint variable) is chosen to be the oxygen coordination number of the first solvation shell, which is 4 for Ag^{+}_{aq} and 5 for Ag^{2+}_{aq}. We show that if the external chemical potential μ is set to the reaction free energy obtained for the same model system using an alternative grand canonical scheme then the reduced species can be oxidized at zero cost in reversible work, confirming the consistency of our grand canonical method.

1. Introduction

The electrochemistry of aqueous systems seems almost ideal for the application of ab initio molecular dynamics (MD) methods.[1] In no other area of chemistry are solvent effects and finite temperature fluctuations as crucial as for redox reactions in aqueous solution. The statistical mechanics of redox processes can be studied using suitable classical force field models. (For an example of such a study involving the Fe^{2+}/Fe^{3+} reaction, see ref 2.) However, if the ultimate goal is quantitative comparison to experiment, then the use of fairly high level electronic structure computation is absolutely mandatory, and of course, the electronic structure of solvation complexes is of interest by itself, in particular, in the context of coordination chemistry.

The ultimate goal would be the simulation of redox processes occurring at the anode or cathode in electrochemical cells. Clearly, one of the main difficulties holding such a development back is the familiar problem of system size. Modeling of an interface between a metal electrode and bulk solution is, in terms of the size of the system needed, at the limit of what is currently possible in Car−Parrinello simulation. The first pioneering studies focusing on the structure of the interface[3] have appeared, but no computations of thermochemical or kinetic constants have been attempted (to our knowledge). Fortunately for a subset of electrochemical reactions, both reactant and product remain in solution, which allows for major simplifications. An elementary example of such a reaction is the oxidation of a transition-metal cation M^{n+}, such as the Fe^{2+} ion of ref 2.

$$M^{n+}_{aq} \rightarrow M^{(n+1)+}_{aq} + e^{-} \qquad (1)$$

For this type of reaction, the metal electrodes play the role of catalyst. The electrode in one half-cell collects the electrons produced by the oxidation reaction (the anode), and a second electrode delivers them to the reactants undergoing reduction in the other half-cell (the cathode). However, the metal electrodes play no role in determining the thermodynamic driving force, measured as a potential difference between the electrodes. (For a very readable introduction to the thermodynamics of electrode potentials, see ref 4.)

Catalysts can be of various kinds. This flexibility suggests that for the computation of thermochemical quantities we are free to replace the metal electrode by an electron reservoir, which is more convenient in simulations. This is the basis of the grand canonical extension of the ab initio MD method for the computation of redox potentials that we introduced in ref 5. (A more detailed explanation will be presented in ref 6.) In this approach, the model redox active system interacts with a fictitious electron reservoir at constant electronic chemical potential μ, allowing for the transfer of electrons to and from the system. The free energy of an electrochemical half reaction is determined by sweeping the value of μ, producing an S-shaped curve for the variation of the average number of electrons (the oxidation state) as a function of μ. The value of μ where the system switches over from one oxidation state to the other can be identified with the free energy of oxidation, by close analogy to the titration techniques of the experimentalists for measuring pK_a's.

In the present contribution, we outline an alternative method for estimating the free energy of oxidation that is still based on the same grand canonical ab initio methodology of ref 5. Suppose that we already have a rough estimate of the critical value of μ at which both oxidation states are equally probable. We fix μ at that value and carry the system from the reduced

† Part of the special issue "Hans C. Andersen Festschrift".

* Corresponding author. E-mail: ms284@cam.ac.uk.

10.1021/jp036610d CCC: $27.50
Published on Web 03/02/2004

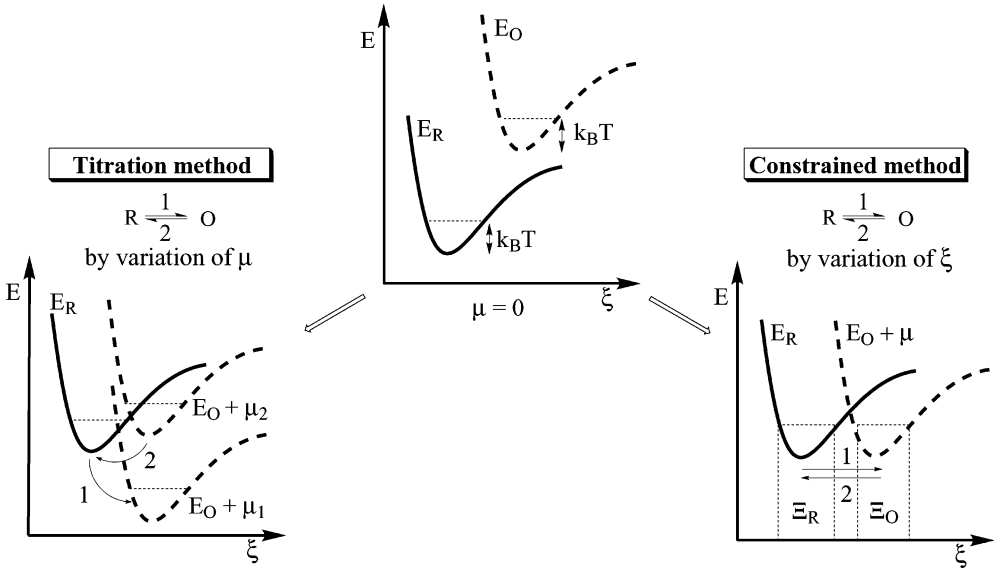

Figure 1. Comparison of two grand canonical simulation methods for the calculation of the free-energy of redox reactions. E_R and E_O denote the potential energy surfaces of the reduced state R and oxidized state O, μ denotes the electronic chemical potential, and $\xi = \xi(\mathbf{R}^N)$ is an order parameter in configuration space. The dotted lines indicate the accessible configuration space at temperature T. In the titration method, the interaction with the electron reservoir effectively shifts the PES of O toward the PES of R by a value of $|\mu|$. The adiabatic forces are derived from the branch lowest in energy. (See eq 2.) The reaction from R to O (1) can occur if $E_O + \mu_1$ is below E_R at an accessible configuration of R. The reaction from O back to R (2) can occur if E_R is below $E_O + \mu_2$ at an accessible configuration of O. Because of relaxation effects, μ_1 and μ_2 can differ significantly. In the constrained MD method, the effective potential is the same composite surface of eq 2, but now the value of μ is fixed (i.e., the PES remains unchanged). The transformation between R and O is enforced by the controlled variation of ξ between the basins of R and O indicated by the intervals Ξ_R and Ξ_O.

to the oxidized state, or vice versa, by a controlled variation of a suitable order parameter. The claim is that the corresponding reversible work as computed by thermodynamic integration gives us the correction that we have to add to the applied μ to obtain the reaction free energy. This method will be applied to one of the oxidation reactions studied in ref 6 using numerical titration, namely, the Ag^+/Ag^{2+} redox reaction in water. As the control variable, we used the oxygen coordination number in the first solvation shell of Ag, which is 4 for the monovalent ion Ag^+_{aq} and 5 for the divalent ion Ag^{2+}_{aq}.

The main objective of this calculation is the validation of the grand canonical ab initio scheme as a numerical tool for to study of electrochemical processes. This scheme is briefly reviewed in section 2. The relation between the reversible work obtained by thermodynamic integration and the free energy of the redox reaction (i.e., the electrode potential) is investigated in section 3, and the application to the Ag aqua ions is discussed in section 4.

2. Ab Initio MD with Variable Numbers of Electrons

2.1. Two Surface MD Schemes. The grand canonical method introduced in ref 5 is, in essence, a two surface simulation of a system of N atoms: One potential energy surface (PES) is the electronic ground-state energy E_R ($\mathbf{R}^N$) of the reduced system R for given atomic positions $\mathbf{R}^N$ and the second PES is the ground-state energy E_O ($\mathbf{R}^N$) of the oxidized system O with one electron less at the same nuclear configuration $\mathbf{R}^N$. Depending on how the vertical ionization energy ΔE ($\mathbf{R}^N$) = E_O ($\mathbf{R}^N$) − E_R ($\mathbf{R}^N$) compares to the applied chemical potential μ the forces driving the ion dynamics are computed from either the reduced or oxidized PES. The result is a composite potential energy surface given by

$$E_\mu(\mathbf{R}^N) = \min[E_R(\mathbf{R}^N), E_O(\mathbf{R}^N) + \mu] \qquad (2)$$

The proof that the PES of eq 2 is the proper effective ionic potential for an open (grand canonical) electronic system in the limit of zero electronic temperature can be found in ref 5. This paper also gives the expression for the force on the ions and technical details concerning the implementation in ab initio MD.

Equation 2 has a rather straightforward interpretation, which is illustrated in Figure 1. Electronic chemical potentials in the condensed phase are negative. As a result, adding a bias μ lowers the PES of the oxidized state with respect to the PES of the reduced state. Hence, although E_O normally lies above E_R (vertical ionization potentials are usually positive), for sufficiently negative μ the surfaces will intersect, creating a region in configuration space where the oxidized system is stable. By lowering μ further, the two basins of stability for R and O will eventually become equivalent. At this point, the system can be with equal probability in either of the two oxidation states. The corresponding configurations will be different in general, and R and O can expected to be separated by a sizable activation barrier as shown in Figure 1.

The reader will have noticed a certain parallel to the surface hopping schemes used in MD studies of excited states. (For an introduction, see ref 7). There are, however, a number of important differences. Both surfaces in the grand canonical method have stable ground-state energies, the difference being the number of electrons, and can in principle be obtained using standard electronic minimization techniques. Furthermore, the dynamics is strictly adiabatic. Therefore, the dynamics of the surface crossing, currently implemented by a brutal switch to the more stable surface (see eq 2),[5,6] has no direct relationship to the actual kinetics of redox reactions in electrochemical cells.

2.2. Free Energy from Numerical Titration. The energy landscape picture sketched in Figure 1 suggests that the value of μ at which the O and R minima become degenerate is special. In the zero-temperature limit, it is equal to the adiabatic ionization energy, and hence, it can be used as a rough estimate of the redox potential. However, solvents are liquids, and the relative stability of the two oxidation states is ultimately

determined by free energies. Fortunately, the double-well picture of Figure 1 can be generalized to finite temperature. It can be shown by rigorous statistical mechanical arguments[5,6] that at a given temperature T the particular value of $\mu := \mu_{1/2}$ for which both oxidation states are equally probable can be identified with the free-energy difference $\Delta A(T)$ between O and R:

$$\Delta A = A_O - A_R = -\mu_{1/2} \tag{3}$$

The (Helmholtz) free energy obtained from the partition function for each single PES is

$$A_M = -k_B T \ln \Lambda^{-3N} \int d\mathbf{R}^N \exp[-\beta E_M(\mathbf{R}^N)] \qquad M = \mathrm{R, O} \tag{4}$$

where in the usual notation $\beta = 1/(k_B T)$. Λ is the average thermal wavelength defined as $\Lambda^{-3N} = \prod_j \lambda_j^{-3N_j}/N_j!$ with λ_j representing the thermal wavelengths $\lambda_j = h/\sqrt{2\pi m_j k_B T}$ of the nuclei species j and N being the total number of nuclei. Because the electronic potential of the reservoir is a fixed parameter under our control, the relation of eq 3 can be used to measure the reaction free energy by varying μ until the system spends equal amounts of time in the reduced and oxidized states. In practice, this means a search for the value of μ where the system changes over from being predominantly in the R state to being in the O state or vice versa.

In ref 5, this method was applied to a molecule (aniline) in vacuum. For finite systems, the free energy of a half reaction can be interpreted as the free energy of ionization. This is more difficult in solution because of the inevitable presence of neutralizing counterions. As in experimental electrochemistry, only relative free energies of half reactions have meaning, and experimental electrode potentials of reactions (eq 1) can be specified only with respect to a suitable reference reaction (e.g., the standard hydrogen electrode). Similarly for our first application of the grand canonical approach to redox reactions in aqueous solution, to be reported in ref 6, we choose two (seemingly) similar half reactions:

$$Ag^+_{aq} \rightarrow Ag^{2+}_{aq} + e^- \tag{5}$$

$$Cu^+_{aq} \rightarrow Cu^{2+}_{aq} + e^- \tag{6}$$

ΔA was estimated to be 1.4 eV for half reaction 5 and -0.3 eV for half reaction 6, giving a free-energy difference of -1.7 eV for the total reaction

$$Ag^{2+}_{aq} + Cu^+_{aq} \rightarrow Ag^+_{aq} + {Cu_{aq}}^{2+} \tag{7}$$

which compares well to the experimental value of -1.83 eV.[8]

2.3. Model System and Size Effects. The computations of ref 6 were carried out using model systems consisting of a single cation and 32 H_2O molecules in a periodic cubic box of size 9.86 Å. There is no explicit counterion. Charge neutrality is imposed by a homogeneous background of opposite charge. Although artificial, this uniform counterion has a decisive technical advantage in grand canonical simulations: the charge can be instantaneously adjusted to a change in the number of electrons without the highly unfavorable insertion of new atomic species in the solution. It will be clear, however, that size effects on the free energy of the half reactions (eqs 5 and 6) will be rather extreme. Fortunately, these size effects largely cancel in the full reaction (eq 7) because the long-range interactions for reactants and products are very similar, involving both a mono- and a dication. This was, in fact, an important consideration in the selection of this model system. We verified that the residual dependence on box size of the reaction free energy of reaction eq 7 has effectively converged within 0.1 eV for the ~10-Å box that was used. For further discussion of the important issue of long-range interactions, we refer to our forthcoming paper.[6]

The work reported here focuses on the statistical mechanics aspect of our method. We will apply a thermodynamic integration scheme, implemented using mechanical constraints, to recompute the free energy of the Ag redox reaction (eq 5). This result will be compared to the 1.4-eV result obtained in ref 6 for exactly the same model system of a Ag cation + 32 solvent molecules, even though this number by itself, being the absolute free energy of a half reaction, has no physical significance.

The technical specifications of the ab initio MD simulation are identical to those in ref 6. The electronic structure calculations for Ag^+_{aq} and Ag^{2+}_{aq} were carried out using the local spin density approximation to DFT (LSDA), the gradient-corrected density functional BLYP,[9,10] Troullier−Martins pseudopotentials[11] for Ag, O, and H, and a plane wave cutoff of 70 Ry. Parametrization and validation of the pseudopotentials can be found in ref 12, where a detailed justification of the choice of the MD system parameters, in particular, the density, is also given. The equilibration and the constrained CPMD runs were carried out using a fictitious electronic mass of 500 au, a time step of 5 au (0.1209 fs), and temperature rescaling to 300 K if the instantaneous temperature exceeded a boundary of 300 ± 50 K. The ab initio MD code that we used was again CPMD[13] with a special extension for the two-surface grand canonical method.[5]

3. Free Energy from Thermodynamic Integration

3.1. Free Energy and Order Parameters. In this section, we describe how the free-energy difference between two oxidation states R and O can be computed using the method of constrained MD.[14,15] In eq 4, the free energies of O and R were defined as exponential integrals of separate energy surfaces E_O and E_R over all configuration space. The idea is to relate these quantities to an integral of the exponent of the composite PES of eq 2 over the two separate parts of configuration space occupied by the reduced and oxidized states. These regions are then bridged by thermodynamic integration. The formalism developed below closely follows that given by Chandler.[16]

To apply thermodynamic integration along a path in configuration space, we first assume that the minima occupied by R and O are sufficiently far apart because we must also allow for thermal fluctuations. This implies that the finite temperature motion of R and O is effectively confined to two separate basins centered around their potential energy minima (Figure 1). These regions can be formally defined by characteristic functions $h_R(\mathbf{R}^N)$ and $h_O(\mathbf{R}^N)$, which are unity for configurations inside and zero outside. The "single-surface" free energy A_M of eq 4 can then be approximated as

$$A^h_M = -k_B T \ln \Lambda^{-3N} \int d\mathbf{R}^N \, h_M(\mathbf{R}^N) \exp[-\beta E_M(\mathbf{R}^N)] \tag{8}$$

A^h_M of eq 8 differs from the free energy in eq 4 by the restriction of the phase-space integral to h_M. Because we have assumed that the weights of all configurations outside h_M are vanishingly small, we can equate A^h_M to A_M.

The next step is to specify the configurational regions h_M in terms of an order parameter ξ, which can be expressed as some (differentiable) function $\xi = \xi(\mathbf{R}^N)$ of the ionic coordinates $\mathbf{R}^N$. The equilibrium values of ξ for R and O are denoted by ξ_R and ξ_O, respectively. To be useful as an order parameter, ξ should

be able to distinguish between h_R and h_O (i.e., the particle coordinates in these regions give values of ξ lying in two nonoverlapping intervals $\Xi_R = [\xi_{R1}, \xi_{R2}]$ and $\Xi_O = [\xi_{O1}, \xi_{O2}]$). The choice of an appropriate order parameter is not always obvious and can become difficult, for instance, if the structures of the reactant and the product are similar. (For a discussion of the complications this can create, see refs 17 and 18.) By introducing the free-energy density[14,16]

$$W_M(\xi') = -k_B T \ln \Lambda^{-3N} \int d\mathbf{R}^N \exp[-\beta E_M(\mathbf{R}^N)]\, \delta(\xi(\mathbf{R}^N) - \xi') \quad (9)$$

the free energy (eq 8) can be written as an integral over ξ:

$$A_M^h = -k_B T \ln \int_{\Xi_M} d\xi' \exp[-\beta W_M(\xi')] \quad (10)$$

The final step consists of replacing the two separate energy surfaces E_M by the PES E_μ of eq 2. The free-energy density corresponding to E_μ is given by

$$W_\mu(\xi') = -k_B T \ln \Lambda^{-3N} \int d\mathbf{R}^N \exp[-\beta E_\mu(\mathbf{R}^N)]\, \delta(\xi(\mathbf{R}^N) - \xi') \quad (11)$$

If the value of μ is chosen so that

$$E_\mu(\mathbf{R}^N) = \begin{cases} E_R(\mathbf{R}^N) & \text{if } \xi \in \Xi_R \\ E_O(\mathbf{R}^N) + \mu & \text{if } \xi \in \Xi_O \end{cases} \quad (12)$$

then we can set $W_O(\xi') = W_\mu(\xi') - \mu$ if $\xi' \in \Xi_O$ and $W_R(\xi') = W_\mu(\xi')$ if $\xi' \in \Xi_R$. The free-energy difference between O and R can now be written as

$$\Delta A^h = A_O^h - A_R^h = -\mu - k_B T \ln \frac{\int_{\Xi_O} d\xi' \exp[-\beta \Delta W_\mu(\xi')]}{\int_{\Xi_R} d\xi' \exp[-\beta \Delta W_\mu(\xi')]} \quad (13)$$

where $\Delta W_\mu(\xi') = W_\mu(\xi') - W_\mu(\xi_R)$ is the reversible work on the PES E_μ, evaluated by integrating the corresponding mean force (see the next section). Thus, whereas in the grand canonical ensemble the transition between oxidation states was made by varying μ (i.e., by transformation of the effective PES), here the transition is enforced by varying the configurational constraint ξ from ξ_R to ξ_O on the PES E_μ with μ being a constant (Figure 1).

The margins for appropriate values of μ appear to be fairly flexible provided the thermal basins of O and R occupy distinct regions in configuration space. What should be avoided is a situation in which the intersection of the $E_O + \mu$ and E_R surfaces comes within the range of the thermal fluctuations in either basin (Figure 1). In practice, we take μ from the interval $\max(\Delta E_O) < |\mu| < \min(\Delta E_R)$ where ΔE_O and ΔE_R are the vertical ionization energies and $\Delta E_M = E_O - E_R$ is obtained along an unconstrained trajectory of the oxidized (M = O) and reduced (M = R) system. This choice of μ satisfies the conditions stated in eq 12. In this context, we also point out that the method of merging the two PESs for the oxidation states in a single surface E_μ is more generally applicable and not limited to only thermodynamic integration techniques. To make this abundantly clear we have made the somewhat tedious distinction between the characteristic functions h_M and the description by an order parameter ξ.

3.2. Free Energy and Mechanical Constraints. In the molecular dynamics method, configurational averages are computed as averages over a trajectory in phase space. The MD estimator for the reversible work function (eq 11) is therefore obtained from the phase-space integral

$$W_\mu(\xi') = -k_B T \ln \int d\mathbf{R}^N d\mathbf{p}^N \exp[-\beta \mathcal{H}_\mu(\mathbf{p}^N, \mathbf{R}^N)]\, \delta(\xi(\mathbf{R}^N) - \xi') \quad (14)$$

with the Hamiltonian $\mathcal{H}_\mu(\mathbf{p}^N, \mathbf{R}^N) = K(\mathbf{p}^N) + E_\mu(\mathbf{R}^N)$. In principle, the free-energy profile $\Delta W_\mu(\xi')$ can be computed directly from the mean force:[16]

$$\Delta W_\mu(\xi') = \int_{\xi_R}^{\xi'} d\xi'' \frac{d}{d\xi''} W_\mu(\xi'') = \int_{\xi_R}^{\xi'} d\xi'' \left\langle \frac{\partial \mathcal{H}_\mu}{\partial \xi} \right\rangle_{\xi''}^{\text{cond}} \quad (15)$$

where the notation $\langle O \rangle_{\xi'}^{\text{cond}}$ indicates the conditional (cond) ensemble average of a phase-space function $O(\mathbf{R}^N, \mathbf{p}^N)$,

$$\langle O \rangle_{\xi'}^{\text{cond}} = \frac{\int d\mathbf{p}^N d\mathbf{R}^N \exp[-\beta \mathcal{H}_\mu(\mathbf{p}^N, \mathbf{R}^N)]\, \delta(\xi(\mathbf{R}^N) - \xi')\, O(\mathbf{R}^N, \mathbf{p}^N)}{\int d\mathbf{p}^N d\mathbf{R}^N \exp[-\beta \mathcal{H}_\mu(\mathbf{p}^N, \mathbf{R}^N)]\, \delta(\xi(\mathbf{R}^N) - \xi')} \quad (16)$$

which can be evaluated by imposing the order parameter $\xi(\mathbf{R}^N)$ as a mechanical constraint.[14] However, in most recent MD implementations of thermodynamic integration, the $-\langle \partial \mathcal{H}_\mu / \partial \xi \rangle_{\xi''}^{\text{cond}}$ force is not evaluated by explicit computation of the derivative of the total energy with respect to the order parameter but is estimated by the Lagrange multiplier λ obtained from the constrained run:[15]

$$\left\langle \frac{\partial \mathcal{H}_\mu}{\partial \xi} \right\rangle_{\xi'}^{\text{cond}} \approx -\langle \lambda \rangle_{\xi'}^{t} \quad (17)$$

The superscript t denotes a time average over a trajectory constrained at the value ξ' of the order parameter given by the subscript. The total force $\mathbf{F}_I^{\text{tot}}$ on the ion I is given by

$$\mathbf{F}_I^{\text{tot}} = \mathbf{F}_I + \mathbf{F}_I^{\text{c}} \quad (18)$$

$$\mathbf{F}_I = -m_I \frac{\partial E_\mu(\mathbf{R}^N)}{\partial \mathbf{R}_I} \quad (19)$$

$$\mathbf{F}_I^{\text{c}} = -\lambda \frac{\partial \xi(\mathbf{R}^N)}{\partial \mathbf{R}_I}\Big|_{\xi'} \quad (20)$$

This relation (eq 17) is approximate and requires a number of corrections. An exact expression of eq 17 is given in ref 15. In practice, these corrections are minor and are usually omitted. (For an explicit evaluation of these corrections in a specific example, see ref 19.)

4. Application to the Ag^+/Ag^{2+} Redox Couple

4.1. Coordination-Constrained Molecular Dynamics. To apply the scheme developed in section 3 to the redox reaction of the silver aqua ion (eq 5), we must first decide on a suitable order parameter distinguishing between the two oxidation states. The Ag aqua ion, at the close of the d-block transition series, forms highly fluxional coordination complexes undergoing continuous rearrangement even on the MD time scale.[6,12] The coordination shell of Ag_{aq}^+ has, on average, the geometry of a distorted tetrahedron, in agreement with neutron-diffraction

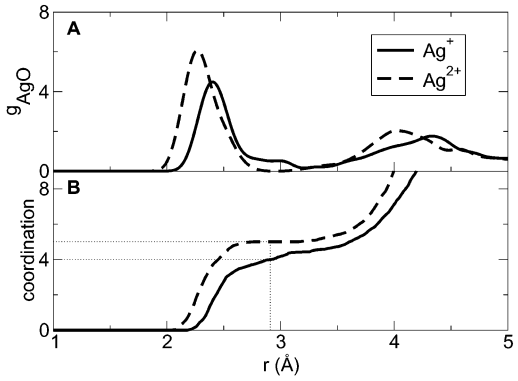

Figure 2. (A) Oxygen−metal ion radial distribution function (RDF) g_{AgO} for Ag_{aq}^{+} and Ag_{aq}^{2+}. (B) Spherical integration of g_{AgO} gives the oxygen coordination number of Ag. The RDF was obtained from a 3-ps trajectory. The radius of the first solvation shell is defined by the location of the first minimum of g_{AgO}, which is a little below 3.0 Å for both ions. The RDF integrates to 4 for Ag_{aq}^{+} and to 5 for Ag_{aq}^{2+} at a radius of 2.91 Å (dashed lines). This well-defined structural difference enables us to use the oxygen coordination number at 2.91 Å as a reaction coordinate for the transformation between Ag_{aq}^{+} and Ag_{aq}^{2+}.

measurements[20,21] and optical studies.[22] Four-fold coordination is also regarded to be the solvation structure of Ag^{+} in polycrystalline ice.[23] The Ag−O coordination distances of water clusters of Ag_{aq}^{+} were investigated previously in our group[12] and found to be in good agreement with MP2 calculations of ref 24. The first peak of the radial distribution function (RDF) of aqueous Ag_{aq}^{+} (Figure 2) is centered at 2.35 Å, which is in the range of experimental results, 2.32−2.43 Å.[20,21] Aqueous Ag_{aq}^{2+} forms a distorted trigonal bipyramid that occasionally transforms to a shape approximating a square pyramid. As one can see in Figure 2, the Ag−O bond length is on average 0.1 Å smaller than for Ag_{aq}^{+}. The coordination number as defined in eq 21 varies between 3.2 and 4.6 for Ag_{aq}^{+} and between 4.9 and 5.0 for Ag_{aq}^{2+}. Despite the thermal fluctuations, the difference in the number of solvent molecules in the first coordination shell is sufficiently well defined to be able to discriminate between Ag_{aq}^{+} and Ag_{aq}^{2+}. Therefore, we have chosen the oxygen coordination number of Ag as the order parameter for the constrained MD method. (See, however, the discussion in section 4.2.)

For application as a mechanical constraint, the coordination number must be expressed as a differentiable (smooth) function of the coordinates. In an earlier technical publication,[25] we showed that the sharp distance criterion used to determine coordination numbers can be relaxed with the help of a Fermi function. Following this same approach here, we define the oxygen−silver coordination number order parameter as

$$\xi(\mathbf{R}^N) = \sum_O S(|\mathbf{R}_O - \mathbf{R}_M|) \tag{21}$$

with S being the Fermi function

$$S(|\mathbf{R}_O - \mathbf{R}_M|) = \frac{1}{\exp[\kappa(|\mathbf{R}_O - \mathbf{R}_M| - R_c)] + 1} \tag{22}$$

In eq 21, O runs over all oxygen atoms, and the index M denotes the Ag atom. $S = 1$ for oxygen atoms that are well within the radius $R < R_c$ with respect to the metal atom. Similarly, for large distances $S = 0$. Oxygen atoms that are approximately at a distance R_c from the metal atom are assigned fractional weight. The width of this region can be adjusted by the parameter κ. The cutoff radius $R_c = 2.91$ Å was chosen so that the RDF obtained from an unconstrained trajectory integrates to 4 for Ag_{aq}^{+} and to 5 for Ag_{aq}^{2+} (Figure 2). With a value of 10 $Å^{-1}$ for κ, the coordination number of an equilibrium configuration taken from an unconstrained trajectory is $\xi_R = 3.94$ for Ag_{aq}^{+} and $\xi_O = 4.97$ for Ag_{aq}^{2+}. This should be compared to the coordination numbers of these configurations obtained by counting the oxygen atoms within the radius R_c, which are exactly 4 and 5. The discrepancy is due to the finite width of the Fermi function, which cannot be taken as infinitely small because then the force on an atom at position R_c would diverge. Similar order parameters have been used with success in the study of water autodissociation[19] and the computation of the pK_a of a weak acid (pentahydroxyphosphorane).[26]

The parameter μ for the effective PES E_μ was deliberately fixed at the negative of the free-energy difference reported in ref 6, $\mu := -1.38$ eV. This choice fulfills the conditions on μ stated in eq 12. Every 10 CPMD steps, the wave function was quenched to the Born−Oppenheimer surface, yielding the optimized instantaneous energies of the reduced and oxidized states. With this input, E_μ was calculated according to eq 2, and the ionic forces for the next 10 CPMD steps were determined according to eq 18. The force of eq 19 was derived from the PES E_R if $E_\mu = E_R$ and from E_O otherwise. The constraint force of eq 20 (for an explicit expression, see ref 25) was computed and used to obtain the Lagrange multiplier λ by applying the velocity Verlet version of the SHAKE algorithm.[27] The time average $\langle\lambda\rangle_{\xi'}^{t}$ was evaluated for a limited series of values of ξ between $\xi_R = 3.94$ and $\xi_O = 4.97$. The runs were carried out sequentially, which means that the run at a value ξ_i was initiated using the final configuration of the run at the previous value ξ_{i-1}.

4.2. Results and Discussion. The results for the mean force $\langle\lambda\rangle_{\xi'}^{t}$ and the corresponding free-energy profile obtained by numerical integration are shown in Figure 3. The average of the Lagrange multiplier used as an estimate for the mean force is typically a few hundredths of an electronvolt, but the fluctuations of this quantity as measured by the root-mean-square deviation are 1 to 2 orders of magnitude higher (between 0.3 and 2.0 eV depending on the value of ξ). Combined with the limited length of the MD trajectories (typically 1−3 ps for each value of the constraint), this leads to a sizable statistical error in the free-energy profile, estimated to be on the order of 0.2 eV. The accuracy of the data, however, is sufficient to support the central statement of this work: the reversible work required to transfer the system from the reduced to the oxidized state vanishes for $\mu = \mu_{1/2}$. Moreover, the sign of the average Lagrange multiplier follows the expected trend. The system responds to an increase in the coordination from $\xi_R = 3.94$ to 4.5 with a negative mean force reaching a minimum of −0.1 eV at $\xi = 4.5$. In this interval of ξ values, the system remains in the reduced state. The applied constraint pulls oxygen atoms of the second solvation shell into the first against the repulsive forces because of overcrowding. This explains the negative sign of $\langle\lambda\rangle_{\xi'}^{t}$. Further increases of the constraint make the oxidized state more favorable. The reaction system switches from R to O 200 fs after increasing the constraint to $\xi = 4.7$. During the remainder of this run, the system stays in the oxidized state and relaxes toward the trigonal-bipyramidal coordination of Ag_{aq}^{2+}. To maintain the constraint value of 4.7, the constraint force now has to push a water molecule of the preferred 5-fold solvation sphere away from the coordination center. Consequently, $\langle\lambda\rangle_{\xi'}^{t}$ changes sign and peaks at a value of 0.1 eV at ξ

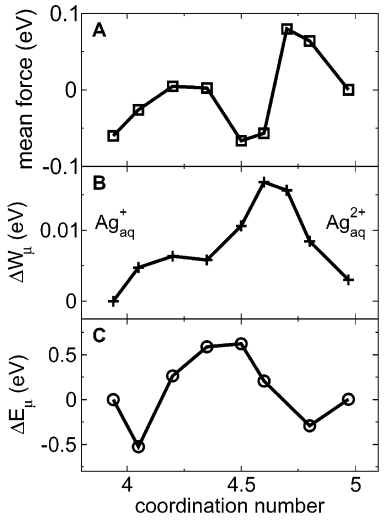

Figure 3. Mean force $\langle\lambda\rangle^t_\xi$ of eq 17 (A), the corresponding free-energy profile of eq 15 (B), and the average potential energy difference (C) calculated for the transformation of Ag^+_{aq} (R) to Ag^{2+}_{aq} (O) (eq 5) under conditions of a fixed electronic chemical potential of $\mu = -1.38$ eV. The differences in the free-energy density ΔW_μ and the average potential energy ΔE_μ are set equal to zero at $\xi = 3.94$. The reaction coordinate ξ is defined in eq 21 as the oxygen coordination number of Ag at $R_c = 2.91$ Å and $\kappa = 10$ Å^{-1} (Figure 2). The equilibrium value of ξ is 3.94 ($= \xi_R$) for Ag^+_{aq} and 4.97 ($= \xi_O$) for Ag^{2+}_{aq}. Integrating $-\langle\lambda\rangle^t_\xi$ between ξ_R and ξ_O gives reversible work of $\Delta W_\mu(\xi_O) = 0.0 \pm 0.2$ eV. The reaction from R to O occurs at a constraint value of 4.7, as can be seen from the change in the sign of $\langle\lambda\rangle^t_\xi$.

$= 4.7$. At $\xi_O = 4.97$, the system has fully settled in the equilibrium configuration of Ag^{2+}_{aq}.

Integrating the negative of mean force $-\langle\lambda\rangle^t_{\xi'}$ between ξ_R and ξ_O yields net reversible work of $\Delta W_\mu(\xi_O) = 0.0 \pm 0.2$ eV for the transformation of the reduced state to the oxidized state. Neglecting the small contributions of thermal fluctuations around equilibrium (i.e., setting the thermal width parameters Ξ_R and Ξ_O in eq 13 equal to zero), we find an approximate free energy of oxidation

$$\Delta A^h \approx -\mu + \Delta W_\mu(\xi_O) \tag{23}$$

which is virtually identical to the negative of the chemical potential μ of the electron reservoir. Because $-\mu = 1.38$ eV was chosen to be equal to ΔA of reaction 5, which was estimated from the variation of μ in ref 6, the results of Figure 3 can be taken as a strong confirmation of our grand canonical approach.

Unfortunately, the reaction from the product back to the reactant failed to occur when ξ was decreased from ξ_O to ξ_R. The effective PES of the oxidized state, $E_O + \mu$, never rose above the PES of the reduced state, E_R, for all values of the constraint variable between 4.97 and 4.2, keeping the system in the oxidized state. Rather than reverting to the tetrahedral equilibrium structure of Ag^+_{aq}, the coordination of Ag^{2+}_{aq} had evolved at $\xi = 4.2$ into a square-planar conformation, which proved to be (meta) stable against reduction. Interpreted in terms of a (free) energy landscape picture, this result suggests that the path leading to the metastable, planar four-coordinated Ag^{2+}_{aq} ion is an easier route out of the basin of the Ag^{2+}_{aq} complex than the path back to the four-coordinate Ag^{1+}_{aq} monocation. Thus, whereas the coordination number is suitable as an order parameter distinguishing between the basins of the stable four-coordinate Ag^{1+}_{aq} and five-coordinate Ag^{2+}_{aq} species (recall section 4.1), it fails to discriminate between oxidation states in general. This behavior, typical for a complex multi-minimum energy landscape, can be seen as a consequence of the well-known structural flexibility of Ag ions. (See, for example, ref 28.)

A more puzzling observation is the small barrier height of only $0.7k_BT$ suggesting that Ag^+_{aq} and Ag^{2+}_{aq} are unstable states in dynamical equilibrium at $\mu = \mu_{1/2}$ and room temperature. This also would imply that the reaction path may be sampled reversibly even on the picosecond time scale of the simulation, in contradiction with the results obtained from equilibrium simulations that clearly show that the interval of the coordination number of Ag^+_{aq} does not overlap with the corresponding interval of Ag^{2+}_{aq}. In addition, a coordination number of 4.7 that is required to transform Ag^+_{aq} to Ag^{2+}_{aq} was not observed in equilibrium simulations of several picoseconds. To reconcile these conflicting observations, we note that as consequence of the statistical uncertainties mentioned previously ($\sim$0.2 eV) the calculated height of the free-energy barrier can be underestimated by at least several k_BT, which would explain why spontaneous reactive events are not observed on the short time scale of the simulation. However, the fact remains that the free-energy barrier is unusual small compared to the large interaction energies in the hydration shells of cations. Indeed, the energy barrier of the reaction is calculated to be 0.6 eV, between 1 and 2 orders of magnitude larger than our free maximum (Figure 3). The conclusion must be that entropy effects are significant, effectively canceling the increasing energy. The Ag^+_{aq}/Ag^{2+}_{aq} redox reaction is an example of an inner-sphere reaction in the terminology of Marcus theory. Our results suggest that the transfer of a water molecule from the ordered network of bulk water to the first solvation shell of the redox active ion in such a reaction is associated with large changes in entropy. One could speculate that the competition between entropy and energy also could lead to unusual kinetics that could explain the absence of spontaneous redox reactions in our simulation in spite of the flat free-energy profile.

The problem of the irreversibility of the reaction may have been avoided using advanced reaction-path search methods such as the multicomponent order parameter approach of Laio and Parrinello.[29] A totally unbiased approach such as the transition-path sampling method of the Berkeley group[17,18,30] is perhaps the best guarantee against this type of accident. This method, however, has been designed mainly for the study of reaction mechanisms and kinetics, and the computation of reaction free energies is (still) rather expensive. However, as a way of investigating the mechanism of the insertion and elimination of water molecules in the coordination shell, transition-path sampling is almost ideal, and the application of this method to the redox reaction of silver ions and other group IB aqua ions (Cu, see ref 6)) is a high priority for future research. Such an investigation could also clarify the role of entropy.

5. Conclusions

In this work, we have presented a grand canonical constrained MD method that allows us to calculate free-energy differences between the oxidized and reduced states of an electrochemical half reaction of aqueous solutes. This method was applied to the redox couple Ag^+/Ag^{2+} using a controlled change of the metal coordination to enforce oxidation. The coordination number is an order parameter that is specific to inner-sphere redox reactions. In many redox reactions, in particular, transition-metal ions, the number of coordinated solvent molecules is the same for both oxidation states. However, it will be clear

that our grand canonical method is compatible with any suitable order parameter. Therefore, our approach permits us to study a large variety of redox chemical processes once the structural characteristics of the transformation are known.

The redox reaction takes place on an effective energy surface composed of the PESs of the oxidized and reduced systems shifted with respect to each other by an appropriate energy constant. This offset can be interpreted as the external chemical potential of the electron reservoir. The computed free-energy difference of the Ag^{+}/Ag^{2+} model half reaction agrees with the result reported in ref 6, which is based on a method using the variation of the applied electronic chemical potential ("numerical titration"). The procedures used in both approaches are independent; therefore, the result obtained in this study is a validation of the underlying grand canonical simulation technique. However, in their present implementation both methods suffer from severe sampling problems. A clear manifestation of these problems was the irreversibility of the half reaction when enforced by a change in the coordination number, whereas in the previous study they led to hysteresis between the forward and backward sweeps of the chemical potential.

Although the sampling problems we have encountered are serious, we are confident that they can be resolved by the use of more advanced reaction-path search methods. We therefore conclude that the basis of the grand canonical simulation method that we have developed is sound. This method promises to be a useful tool for the "first principles" investigation of electrochemical processes, which can be regarded as one of the remaining frontiers in computational chemistry.

Acknowledgment. This research was sponsored by EPSRC. J.B. is grateful to the Austrian Academy of Sciences for financial support.

References and Notes

(1) Car, R.; Parrinello, M. *Phys. Rev. Lett.* **1985**, *55*, 2471.
(2) Kuharski, R. A.; Bader, J. S.; D. Chandler, D.; Sprik, M.; Klein, M. L.; Impey, R. W. *J. Chem. Phys.* **1988**, *89*, 3248.
(3) Izvekov, S.; Voth, G. A. *J. Chem. Phys.* **2001**, *115*, 7196.
(4) Compton, R. G.; Sanders, G. H. W. *Electrode Potentials*; Oxford Chemistry Primers; Oxford University Press: Oxford, U.K., 1996; Vol. 41.
(5) Tavernelli, I.; Vuilleumier, R.; Sprik, M. *Phys. Rev. Lett.* **2002**, *88*, 213002.
(6) Blumberger, J.; Bernasconi, L.; Tavernelli, I.; Vuilleumier, R.; Sprik, M. *J. Am. Chem. Soc.*, in press.
(7) Tully, J. C. In *Classical and Quantum Dynamics in Condensed Phase Simulations*; Berne, B. J., Ciccotti, G., Coker, D., Eds.; World Scientific: Singapore, 1998; p 489.
(8) *CRC Handbook of Chemistry and Physics*, 75 ed.; Lide, D. R., Ed.; CRC Press: Boca Raton, FL, 1995.
(9) Becke, A. D. *Phys. Rev. A* **1988**, *38*, 3098.
(10) Lee, C.; Yang, W.; Parr, R. *Phys. Rev. B* **1988**, *37*, 785.
(11) Troullier, N.; Martins, J. *Phys. Rev. B* **1991**, *43*, 1993.
(12) Vuilleumier, R.; Sprik, M. *J. Chem. Phys.* **2001**, *115*, 3454.
(13) *Cpmd*, v3.3a. Hutter, J.; Alavi, A.; Deutsch, T.; Bernasconi, M.; Goedecker, S.; Marx, D.; Tuckerman, M.; Parrinello, M.; MPI für Festkörperforschung and IBM Zurich Research Laboratory: Zurich, 1995−1999.
(14) Carter, E. A.; Ciccotti, G.; Hynes, J. T.; Kapral, R. *Chem. Phys. Lett.* **1989**, *156*, 472.
(15) Sprik, M.; Ciccotti, G. *J. Chem. Phys.* **1998**, *109*, 7737.
(16) Chandler, D. *Introduction to Modern Statistical Mechanics*; Oxford University Press: Oxford, U.K., 1987.
(17) Bolhuis, P. G.; Chandler, D.; Dellago, C.; Geissler, P. L. *Annu. Rev. Phys. Chem.* **2002**, *53*, 291.
(18) Dellago, C.; Bolhuis, P. G.; Geissler, P. L. *Adv. Chem. Phys.* **2002**, *123*, 1.
(19) Sprik, M. *Chem. Phys.* **2000**, *258*, 139.
(20) Skipper, N. T.; Neilson, G. W. *J. Phys.: Condens. Matter* **1989**, *1*, 4141.
(21) Sandström, M.; Neilson, G. W.; Johansson, G.; Yamaguchi, T. *J. Phys. C: Solid State Phys.* **1985**, *18*, 1115.
(22) Texter, J.; Hastreiter, J. J.; Hall, J. L. *J. Phys. Chem.* **1983**, *87*, 4690.
(23) Ichikawa, T.; Li, A. S. W.; Kevan, L. *J. Chem. Phys.***1981**, *75*, 2472.
(24) Martinez, J. M.; Pappalardo, R. R.; Sánchez Marcos, E. *J. Phys. Chem. A* **1997**, *101*, 4444.
(25) Sprik, M. *Faraday Discuss. Chem. Soc.* **1998**, *110*, 437.
(26) Davies, J. E.; Doltsinis, N. L.; Kirby, A. J.; Roussev, C. D.; Sprik, M. *J. Am. Chem. Soc.* **2002**, *124*, 6594.
(27) Andersen, H. C. *J. Comput. Phys.* **1983**, *52*, 24.
(28) Greenwood, N. N.; Earnshaw, A. *Chemistry of the Elements*, 2nd ed.; Butterworth-Heinemann: Woburn, MA, 1997.
(29) Laio, A.; Parrinello, M. *Proc. Natl. Acad. Sci. U.S.A.* **2002**, *20*, 12562.
(30) Bolhuis, P. G.; Dellago, C.; Chandler, D. *Faraday Discuss. Chem. Soc.* **1998**, *110*, 421.